Segmentation of the mouse skull for MRI guided transcranial focused ultrasound therapy planning

T. Hopp[a,b], L. Springer[a,b], C. Gross[a,b], S. Grudzenski-Theis[c,b], F. Mathis-Ullrich[d], and N.V. Ruiter[a,b]

[a]Karlsruhe Institute of Technology, Institute for Data Processing and Electronics, Germany
[b]HEiKA – Heidelberg Karlsruhe Strategic Partnership, Heidelberg University, Karlsruhe Institute of Technology (KIT), Germany
[c]Heidelberg University, University Medicine Mannheim, Department of Neurology, Germany
[d]Karlsruhe Institute of Technology, Institute for Anthropomatics and Robotics, Germany

ABSTRACT

For opening the blood brain barrier using focused ultrasound (FUS) to treat neurodegenerative diseases, mouse-specific therapy planning is an essential step. For our therapy planning approach based on acoustic simulations we here propose to automatically segment the mouse skull and brain from magnetic resonance imaging, which is usually used in combination with FUS for monitoring purposes. The proposed method consists of (1) pre-processing to enhance the image contrast and remove noise, (2) a rough skull segmentation using morphological operations and adaptive binarization, (3) segmentation of the brain using the established 3D-PCNN method, (4) correction of the skull segmentation using the anatomical information about the brain location and (5) a post-processing to remove obvious errors from the final skull segmentation. The method is evaluated with four in-vivo datasets obtained with different parameters. The median Matthews Correlation Coefficient (MCC) on all slices of four datasets was 0.85 for the brain segmentation, 0.69 for the overall skull segmentation and 0.78 for the skull cap. Finally for showcasing the application an acoustic simulation based on the segmentation is presented, which results in a comparable prediction of the pressure field prediction as our earlier method based on micro-CT, and lines up well with literature estimations of the ultrasound attenuation.

Keywords: Skull segmentation, magnetic resonance imaging, subject-specific therapy planning, focused ultrasound, blood brain barrier opening

1. INTRODUCTION

Focused ultrasound (FUS) provides novel opportunities for targeted treatment of diseases. One particularly promising application is using FUS for blood brain barrier opening (BBBo) in a non-invasive and safe way[1] to treat various neurological diseases by dedicated medication. In our research we are especially interested in the cell-mediated therapy of neurological diseases, which is currently being investigated in animal studies with mice. The integration of small animal magnetic resonance imaging (MRI) guidance (MRgFUS) enables monitoring of the FUS application.

There is a delicate window of acoustic parameters, within which a BBBo can be obtained, while at the same time minimizing irreversible damage to brain tissue.[2] Targeting this window is especially challenging since a trans-cranial application of FUS leads to severe attenuation and distortion of the ultrasound wave. In order to provide safe and robust BBBo, therapy planning is an essential process before in-vivo application. Due to the variability in the anatomy of mice depending e.g. on age, weight and type, this therapy planning will be in best case performed for each subject individually, i.e. by taking into account the individual anatomy of each mouse. We developed a simulation framework based on acoustic simulations[3] in order to optimize the FUS parameters before in-vivo application. The simulation is able to include a model of the skull and brain and predicts the pressure field in the focal spot inside the brain.

Contact: torsten.hopp@kit.edu

Figure 1. Processing steps from left to right: original MRI slice, after pre-processing, initial skull segmentation, brain segmentation, corrected skull segmentation, after post-processing

A missing link between individual therapy planning and in-vivo application is however the automated extraction of the skull and brain anatomy of each mouse. During in-vivo procedures often only MRI is available as imaging modality. Hence for automation of the individual therapy planning, automatic segmentation of the mouse skull and brain in pre-sonication MRI scans is necessary to derive an anatomical model for acoustic simulations.

The segmentation of the mouse skull in MRI is challenging, because bone results in low signals in MRI and can only be imaged indirectly in conventional MR series. Most methods for MRI segmentation presented until now therefore focus on the segmentation of the brain. Methods are based on neural networks, e.g.,[4–6] or based on traditional image processing methods like e.g. graph-based segmentation.[7] *Wiens et al.*[8] presented an approach to automatically segment complex bone structures of rodents in micro-CT scans. Several approaches exist for segmenting the human skull in MRI images, e.g. *FSL BET2*,[9] using the *SPM12*[10] suite, and *BrainSuite*,[11] of which performances are compared in *Nielsen et al.*[12] Only few approaches addressing the problem of segmenting the skull in MRI of rodents have been published: e.g. *Wang et al.*[13] presented an approach based on K-means clustering and level sets, however using a manual interaction by the user.

In this paper we present a novel method for automated segmentation of the mouse skull cap and brain in T2 weighted MRI images. These segmentations are subsequently used to showcase acoustic simulations of a dedicated FUS system for therapy planning.

2. METHODS

For acoustic simulations of trans-cranial applications we are most interested in precisely segmenting the skull cap. The proposed method to perform such a segmentation is based on a multi-step approach (Figure 1): (1) pre-processing is applied to enhance the image contrast and remove noise, (2) the skull is roughly segmented using morphological operations and adaptive binarization, (3) the brain is segmented using the established 3D-PCNN method,[4] (4) the skull segmentation is refined using the anatomical information about the brain location, (5) post-processing is applied to remove obvious outliers and errors. Beside the brain segmentation in step 3, the procedure is performed for each two dimensional slice separately. We detail these methods in the following paragraphs.

For preprocessing, the image contrast is adjusted using a contrast limited adaptive histogram equalization[14] followed by a histogram stretching. Due to the short acquisition times at very high resolutions in the underlying MRI, images are considerably noisy. To reduce the noise we apply a non-local means filtering with a search window and neighborhood, which were empirically optimized.

The skull segmentation first identifies areas potentially representing bone, which are characterized by a low signal in MRI. For this purpose we use a morphological background removal with a closing operation and a structured element in the shape of a disk, which was selected due to the approximately round shape of the mouse head. To retrieve the dark structures, this closed image is subtracted from the preprocessed one. The resulting image is binarized using Otsu's method[15] and holes in the mask are closed by morphological closing. The increase in object size by the closing operation is filtered out by intersecting the mask with an inverted adaptive binarization of the original slice. As the skull is now mostly represented as a continuous object in the resulting mask we analyze the connectivity of pixels and extract the n largest segments, which are the candidates for skull regions. Empirically, $n = 4$ lead to good results given the available data.

Segmenting the brain in the MRI is important for modeling anatomically correct brain tissue in the acoustic simulation. Moreover, the anatomical information can be used to identify a region of interest (ROI) in which the

skull can be expected. We make use of a bias field correction using multiplicative intrinsic component optimization (MICO)[16] followed by applying the 3D-PCNN method,[4] a neural network based method to segment the brain in volumetric MRI. To remove wrongly segmented regions outside the brain we make use of the observation that the brain is usually the largest segmented object in the center of the mouse head in each slice. The segmentation mask representing the brain is therefore selected by extracting the connected object in which the center of mass of the mask is located.

The brain segmentation is then used to create a ROI around the outer surface of the brain by dilation of $0.7\,mm$ according to the maximum skull thickness that can be expected in mice.[17] This ROI is intersected with the candidates for the skull region. To control this operation we calculate the Feret diameter[18] of each of the segments and remove outliers by selecting only objects with a Feret diameter $> 0.4\,mm$. We furthermore make use of the continuity of the skull across slices and therefore only keep segments, which overlap with segments in the neighboring slices. Finally small gaps in the skull cap are closed.

To showcase the use of the segmented skull and brain for therapy planning we applied our previously developed 3D acoustic simulation based on k-Wave.[19] An eight element bowl-shaped FUS transducer corresponding to a model of IMASONIC Inc., France, has been modeled and the skull and brain segmentation have been used to model the anatomy of a mouse head with material parameters from literature.[3] For this purpose the skull is interpolated to isotropic resolution of $0.1\,mm$ using a nearest neighbor interpolation.

3. RESULTS

For evaluation of the automated segmentation we used in total four datasets. All MRI volumes were acquired on a 9.4T BioSpec 94/20 USR small animal system (Bruker, Germany). Two T2-weighted images were acquired using a 2D transversal Rapid Acquisition with Relaxation Enhancement (RARE) sequence with the following parameters: repetition time (TR)/echo time (TE) = $2500/33\,ms$, matrix size = 256 x 256, 16 slices with slice thickness = $0.8\,mm$, spacing between slices = $1.0\,mm$, in-plane resolution = $0.0781\,mm \times 0.0781\,mm$, number of averages = 2. A third MRI volume was acquired on the same device with the same parameters except for slice thickness = $0.4\,mm$, spacing between slices = $0.5\,mm$ and 29 slices in total and a fourth dataset was acquired at 512×512 matrix size, $0.043 \times 0.043\,mm$ resolution and 12 slices at $0.5\,mm$ slice thickness and $1\,mm$ spacing between slices. The datasets thereby represent a heterogeneous ensemble of images to evaluate the robustness of the proposed approach.

Figure 2 shows a qualitative representation of the segmentation for one exemplary dataset in comparison to the reference data. Green areas indicate that the segmentation overlaps with reference data, red indicates pixels falsely classified as skull, blue indicates pixels, which are part of the reference data but are missing in the segmentation using the proposed method. Visually, the segmentation agrees well with the reference data, especially the skull cap. Most deviations from the reference data can be observed at lateral regions of the skull near the temporomandibular joint.

For all datasets an expert annotated the skull and the brain manually in all slices using MITK.[20] Matthews Correlation Coefficient (MCC)[21] was calculated to quantitatively evaluate the quality of the skull, respectively, brain segmentation. The automatic segmentation was performed 1000 times and results were averaged for each dataset since the brain segmentation step produces a non-deterministic result. The median MCC score on all slices of four datasets was 0.85 for the brain segmentation, 0.69 for the overall skull segmentation, and 0.78 for the skull cap. In average this indicates a good agreement of automated segmentation and reference data.

There were differences in the performance for the four datasets (Figure 3). The segmentation of the datasets 1 and 2, which have been acquired with the same parameters result in comparable MCC for the brain, the whole skull, and the skull cap. The brain segmentation in datasets 3 and 4 reached a MCC slightly lower though still at a good agreement with the reference data. While in dataset 3 the whole skull and skull cap segmentation are not affected by this slight decrease in brain segmentation accuracy, dataset 4 interestingly showed a considerably lower MCC for the whole skull and skull cap. We believe this decrease is the result of the considerably higher noise in the dark regions of the images due to the higher resolution of the dataset.

The computation time for a single segmentation is in the range of a few seconds, depending on the number of slices and the matrix size. For a 256 x 256 matrix size the average computation time per slice on a desktop

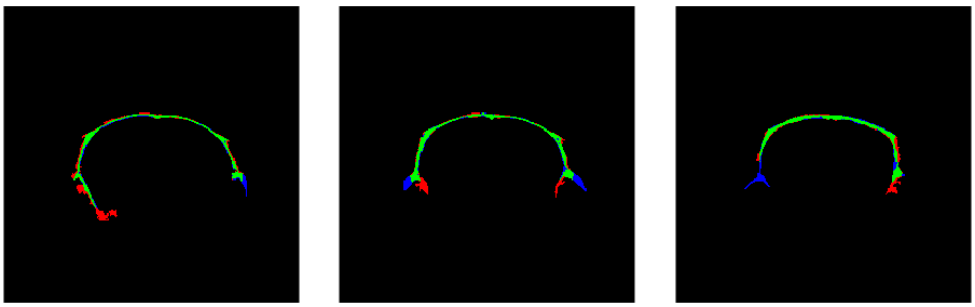

Figure 2. Exemplary output of the automatic skull segmentation for three consecutive slices of one dataset. Green: segmentation overlapping with reference data, red: falsely positive classified pixels, blue: pixels of reference data missing in automatic segmentation.

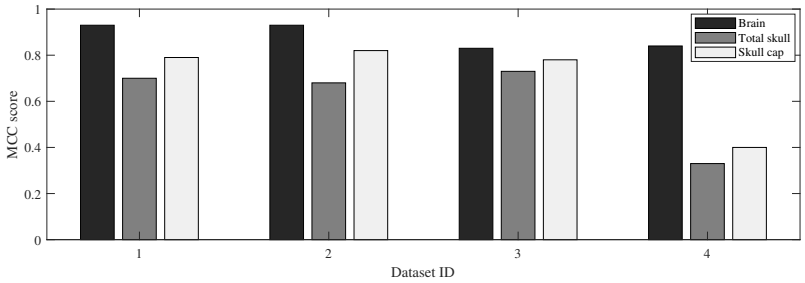

Figure 3. Median MCC scores for brain, total skull and skull cap segmentation of the four evaluated datasets.

PC (Intel Core i7-9700K at 3.60 GHz and 32GB DDR4 RAM) was 0.6 s, for a 512 x 512 matrix size 4.6 s using a MATLAB implementation. Around 80% of the computation time is spent for the 3D-PCNN method.

Figure 4 shows an exemplary result of an acoustic simulation based on the segmented skull and brain derived by the proposed segmentation method. The peak sound pressure in the brain in this simulation was 0.57 MPa in comparison to 0.76 MPa for a simulation in water only. Thereby the transmission factor through the skull was approx. 75.1%. Compared to a simulation with a mouse skull extracted from a micro CT scan of a mouse approximately the same age and type[3] in which we simulated and verified an attenuation of approx. 76%, the result using the segmented MRI is well in line. Also compared to literature, in which the transmission factor through rat skulls has been evaluated as a function of the skull thickness, the presented results are agreeing well.[22]

4. DISCUSSION AND CONCLUSION

To our best knowledge this work presents the first method for fully automated simultaneous skull and brain segmentation in MRI images of mice. The method is based on traditional image processing methods and does not require e.g. labeled data for training. Though a limited number of datasets has been used for evaluation, the results are promising: upon visual inspection, segmentations agree well with manual segmentations that served as reference data. The method has been applied to different MRI protocols and provided basic robustness for brain and skull cap segmentation while it can be noticed that low noise in the MRI images enhances the results. For in-vivo application we therefore recommend to use MRI protocols that comply approximately with the evaluated datasets 1, 2 or 3.

Using the automated segmentation in combination with our acoustic simulation framework for therapy planning lead to reasonable results in terms of the loss in sound pressure due to the penetration through the skull cap. Though the distance between slices was large in MRI images, which results in staircasing artifacts (see Figure 4), the results are comparable to using a considerably higher resolution micro CT dataset.

In conclusion the presented method is an essential step for fully automated subject-specific therapy planning in future in order to robustify BBBo procedures at a safe level.

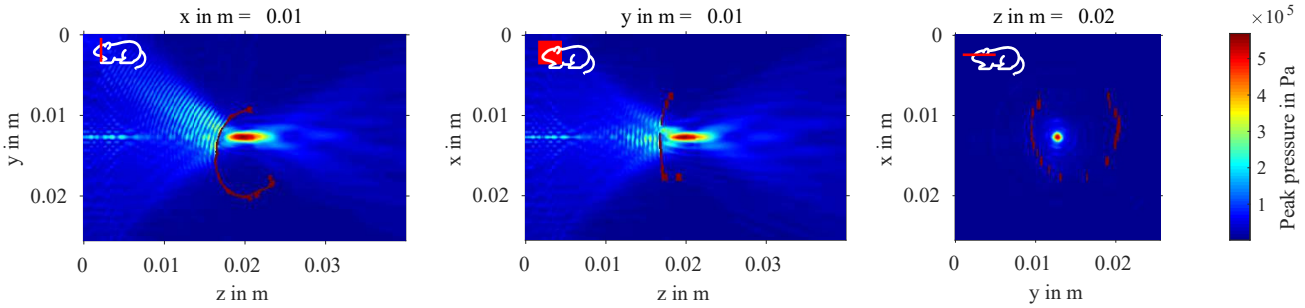

Figure 4. 3D acoustic simulation based on skull and brain segmented from an MRI. The skull is displayed in dark red for reference. Left to right: transversal, sagittal and coronal plane. In transversal and sagittal plane the FUS transducer is located on the left. In sagittal and coronal plane staircasing due to large distance between slices can be recognized, though this does not have a major effect on the distortion of the focal area.

REFERENCES

[1] Hynynen, K., McDannold, N., Vykhodtseva, N., and Jolesz, F. A., "Noninvasive mr imaging-guided focal opening of the blood-brain barrier in rabbits," *Radiology* **220**(3), 640–646 (2001).

[2] Magnin, R., Rabusseau, F., Salabartan, F., Mériaux, S., Aubry, J., et al., "Magnetic resonance-guided motorized transcranial ultrasound system for blood-brain barrier permeabilization along arbitrary trajectories in rodents," *Journal of therapeutic ultrasound* **3**, 22 (2015).

[3] Gross, C., Hopp, T., Grudzenski-Theis, S., Heger, S., Fatar, M., and Ruiter, N. V., "Towards subject-specific therapy planning for non-invasive blood brain barrier opening in mice by focused ultrasound," in [*Proceedings 2021 IEEE International Ultrasonics Symposium (IUS)*], 1–4 (2021).

[4] Chou, N., Wu, J., Bingren, J. B., Qiu, A., and Chuang, K.-H., "Robust automatic rodent brain extraction using 3-d pulse-coupled neural networks (PCNN)," *IEEE Transactions on Image Processing* **20**(9), 2554–2564 (2011).

[5] Hsu, L.-M., Wang, S., Ranadive, P., Ban, W., Chao, T.-H. H., Song, S., Cerri, D. H., Walton, L. R., Broadwater, M. A., Lee, S.-H., Shen, D., and Shih, Y.-Y. I., "Automatic skull stripping of rat and mouse brain MRI data using u-net," *Frontiers in Neuroscience* **14** (2020).

[6] Roy, A. G., Conjeti, S., Navab, N., and Wachinger, C., "QuickNAT: A fully convolutional network for quick and accurate segmentation of neuroanatomy," *NeuroImage* **186**, 713–727 (2019).

[7] Oguz, I., Zhang, H., Rumple, A., and Sonka, M., "RATS: Rapid automatic tissue segmentation in rodent brain MRI," *Journal of Neuroscience Methods* **221**, 175–182 (2014).

[8] Wiens, V., "Volumetric segmentation of complex bone structures from medical imaging data using reeb graphs," in [*Proceedings of CESCG 2013 - The 17th Central European Seminar on Computer Graphics*], 113–120 (2013).

[9] Pechaud, M., Jenkinson, M., and Smith, S., "Bet2 - mri-based estimation of brain, skull and scalp surfaces," tech. rep., FMRIB Technical Report TR06MP1 (2006).

[10] The FIL Methods Group, *SPM12 Manual*.

[11] Dogdas, B., Shattuck, D. W., and Leahy, R. M., "Segmentation of skull and scalp in 3-d human MRI using mathematical morphology," *Human Brain Mapping* **26**(4), 273–285 (2005).

[12] Nielsen, J. D., Madsen, K. H., Puonti, O., Siebner, H. R., Bauer, C., Madsen, C. G., Saturnino, G. B., and Thielscher, A., "Automatic skull segmentation from MR images for realistic volume conductor models of the head: Assessment of the state-of-the-art," *NeuroImage* **174**, 587–598 (2018).

[13] Wang, X., Wang, X., Li, W., and Qian, Z., "Segmentation of scalp, skull, CSF, grey matter and white matter in MRI of mouse brain," in [*2010 3rd International Conference on Biomedical Engineering and Informatics*], IEEE (2010).

[14] Zuiderveld, K., "Contrast limited adaptive histogram equalization," in [*Graphics Gems*], Heckbert, P. S., ed., 474–485, Elsevier (1994).

[15] Otsu, N., "A threshold selection method from gray-level histograms," *IEEE Transactions on Systems, Man, and Cybernetics* **9**(1), 62–66 (1979).

[16] Li, C., Gore, J. C., and Davatzikos, C., "Multiplicative intrinsic component optimization (MICO) for MRI bias field estimation and tissue segmentation," *Magnetic Resonance Imaging* **32**(7), 913–923 (2014).

[17] Ghanbari, L., Rynes, M.L., Hu, J, Schulman, D, Johnson, G.W. et al., "Craniobot: A computer numerical controlled robot for cranial microsurgeries," *Scientific Reports* **9**(1) (2019).

[18] Walter, M. R., [*Stromatolites*], Elsevier Scientific Pub. Co, Amsterdam New York (1976).

[19] Treeby, B. E. and Cox, B. T., "k-wave: MATLAB toolbox for the simulation and reconstruction of photoacoustic wave fields," *Journal of Biomedical Optics* **15**(2), 021314 (2010).

[20] Wolf, I. Vetter M. Wegner I., Nolden, M., Bottger, T., et al., "The medical imaging interaction toolkit (MITK): a toolkit facilitating the creation of interactive software by extending VTK and ITK," in [*Medical Imaging 2004: Visualization, Image-Guided Procedures, and Display*], **5367**, 16 – 27, SPIE (2004).

[21] Matthews, B., "Comparison of the predicted and observed secondary structure of t4 phage lysozyme," *Biochimica et Biophysica Acta (BBA) - Protein Structure* **405**(2), 442–451 (1975).

[22] Gerstenmayer, M., Fellah, B., Magnin, R., Selingue, E., and Larrat, B., "Acoustic transmission factor through the rat skull as a function of body mass, frequency and position," *Ultrasound in Medicine & Biology* **44**(11), 2336–2344 (2018).